MOLECULAR AND CELLULAR BIOLOGY, Aug. 2007, p. 5456–5467 Vol. 27, No. 15
0270-7306/07/$08.00+0 doi:10.1128/MCB.00416-07

Mek1 Kinase Is Regulated To Suppress Double-Strand Break Repair between Sister Chromatids during Budding Yeast Meiosis▽

Hengyao Niu,[1] Xue Li,[2]† Emily Job,[1] Caroline Park,[1] Danesh Moazed,[2] Steven P. Gygi,[2] and Nancy M. Hollingsworth[1]*

Department of Biochemistry and Cell Biology, Stony Brook University, Stony Brook, New York 11794-5215,[1] and Department of Cell Biology, Harvard Medical School, Boston, Massachusetts 02115[2]

Received 9 March 2007/Returned for modification 2 April 2007/Accepted 8 May 2007

Mek1 is a meiosis-specific kinase in budding yeast which promotes recombination between homologous chromosomes by suppressing double-strand break (DSB) repair between sister chromatids. Previous work has shown that in the absence of the meiosis-specific recombinase gene, *DMC1*, cells arrest in prophase due to unrepaired DSBs and that Mek1 kinase activity is required in this situation to prevent repair of the breaks using sister chromatids. This work demonstrates that Mek1 is activated in response to DSBs by autophosphorylation of two conserved threonines, T327 and T331, in the Mek1 activation loop. Using a version of Mek1 that can be conditionally dimerized during meiosis, Mek1 function was shown to be promoted by dimerization, perhaps as a way of enabling autophosphorylation of the activation loop in *trans*. A putative *HOP1*-dependent dimerization domain within the C terminus of Mek1 has been identified. Dimerization alone, however, is insufficient for activation, as DSBs and Mek1 recruitment to the meiosis-specific chromosomal core protein Red1 are also necessary. Phosphorylation of S320 in the activation loop inhibits sister chromatid repair specifically in *dmc1*Δ-arrested cells. Ectopic dimerization of Mek1 bypasses the requirement for S320 phosphorylation, suggesting this phosphorylation is necessary for maintenance of Mek1 dimers during checkpoint-induced arrest.

During the specialized cell division of meiosis, two rounds of chromosome segregation follow one round of chromosome duplication, thereby creating haploid gametes from diploid cells. In the first meiotic division (meiosis I [MI]), homologous chromosomes segregate to opposite poles, while in the second division (MII), sister chromatids segregate to opposite poles. Recombination between nonsister chromatids of homologous chromosomes, combined with sister chromatid cohesion, create physical connections that enable homologs to segregate properly at MI (33). In the absence of these connections, homologous chromosomes disjoin randomly, resulting in chromosomally imbalanced gametes. In humans, the consequences of these nondisjunction events are infertility or birth defects, such as trisomy 21 or Down syndrome (12). While crossovers must occur between homologs during meiosis to be effective for chromosome segregation, in vegetative cells sister chromatids are the preferred templates for DNA repair (19). Determining how the bias in recombination partners changes from sister chromatids to homologs is therefore key to understanding meiosis.

In the budding yeast, *Saccharomyces cerevisiae*, meiotic recombination is initiated by double-strand breaks (DSBs) catalyzed by a meiosis-specific endonuclease, Spo11 (21). The 5′ ends of the DSBs are resected to generate 3′ single-stranded tails, which then invade homologous nonsister chromatids, displacing strands of like polarity. Extension of the invading 3′ tails by DNA repair synthesis proceeds until the displaced strands anneal with 3′ single-stranded tails from the opposite side of the breaks. Further extension and ligation generate double Holliday junction structures that are resolved to make crossovers (2, 36). In addition, a subset of crossovers is created by an alternative pathway using the structure-specific Mus81-Mms4 endonuclease (reviewed in reference 13).

Strand invasion is the critical step that determines partner choice. In vegetative cells, where recombination occurs preferentially between sister chromatids, the recombinase mediating strand invasion is Rad51 (29). In meiotic cells, a meiosis-specific recombinase, Dmc1, is also present (6). Rad51 and Dmc1 colocalize to DSBs and function together in meiotic recombination between homologs (4, 51). *RAD51* facilitates Dmc1 localization to breaks, although the reverse is not true (4, 38). In diploids with *DMC1* deleted, there is no strand invasion of homologs, and as a result, DSBs are unrepaired and hyperresected (6, 16). Furthermore, cells arrest in prophase due to triggering of the meiotic recombination checkpoint (24). Given that Rad51 is present at breaks in *dmc1*Δ mutants and that Rad51 preferentially utilizes sister chromatids as templates for DSB repair in vegetative cells, the fact that DSBs are unrepaired in *dmc1*Δ meiosis suggests that there is a meiosis-specific "barrier to sister chromatid repair" (BSCR) functioning to suppress Rad51-mediated intersister DSB repair.

An important clue to understanding how the BSCR is created came from the discovery that deletion of the meiosis-specific protein kinase Mek1 (also known as Mre4) allows repair of DSBs in *dmc1*Δ diploids (49). Consistent with a role

* Corresponding author. Mailing address: 314 Life Sciences Building, Department of Biochemistry and Cell Biology, Stony Brook University, Stony Brook, NY 11794-5215. Phone: (631) 632-8581. Fax: (631) 632-8575. E-mail: nhollin@ms.cc.sunysb.edu.

† Present address: Amgen Inc., 4000 Nelson Road, Longmont, CO 80503.

▽ Published ahead of print on 25 May 2007.

in the BSCR, *mek1*Δ mutants are specifically defective in interhomolog recombination and, in some genetic assays, exhibit increased sister chromatid recombination (15, 27, 42). An analog-sensitive allele of *MEK1* (*mek1-as*) allows conditional inhibition of Mek1 kinase activity during meiosis. Using this allele, Mek1 kinase activity was shown to be constitutively required after DSB formation in *dmc1*Δ strains to prevent sister chromatid repair (27, 45). Increased Rad51 activity, either by overexpression of *RAD51* or *RAD54* or deletion of a negative regulator of Rad51, *HED1*, suppresses the interhomolog recombination, sporulation, and spore viability defects of *dmc1*Δ (5, 43, 44). This suppression requires Mek1 kinase activity, as inactivation of Mek1-as when *RAD51* is overexpressed in the *dmc1*Δ background results in intersister recombination and dead spores (27). This result indicates that Mek1 does not create a BSCR by directly inhibiting the catalytic activity of Rad51 but instead prevents active Rad51 from invading sister chromatids.

A BSCR is necessary only when DSBs create 3′ single-stranded ends that are faced with the choice of invading either sister chromatids or homologs. Recent experiments suggest that coupling of DSB formation to creation of a BSCR occurs by regulation of Mek1 kinase activity. Mek1 exists in a complex with two other meiosis-specific chromosomal core components, Hop1 and Red1 (3, 40). The last 20 amino acids of Hop1 constitute a functionally distinct region called the C domain that is specifically required for the BSCR (27). Ectopic dimerization of Mek1 suppresses *hop1-K593A* mutant phenotypes, suggesting that the function of the Hop1 C domain in the BSCR is to dimerize Mek1. The Hop1 C domain is phosphorylated in response to DSBs by a kinase other than Mek1, suggesting a mechanism by which DSB formation may be tied to Mek1 activation (27).

Mek1 belongs to the RD family of protein kinases, many of which are activated by phosphorylation of conserved threonines in a portion of the protein called the activation loop (18, 28). Phosphorylation of the activation loop can create conformational changes that allow substrate binding and/or affect the phosphoryl transfer step (1). Modification of activation loop threonines can result either from autophosphorylation (e.g., interleukin-1 receptor-associated kinase 4) or by reaction with another kinase (e.g., cyclin-dependent kinase) (8, 20). For kinases activated by autophosphorylation in *trans*, dimerization is one way to bring the kinase molecules together. Mek1 contains two conserved threonines in its activation loop, T327 and T331. Genetic evidence indicates that T327 phosphorylation is important for Mek1 function during meiosis, but a role for T331 has not been reported (45).

To determine whether T327 and T331 phosphorylation occurs in vivo, mass spectrometry (MS) was used to identify amino acids that are phosphorylated in glutathione *S*-transferase (GST)–Mek1 purified from *dmc1*Δ-arrested cells, where Mek1 kinase activity is constitutively required to prevent intersister DSB repair. In vivo phosphorylation of T327 and T331 was confirmed. T327 phosphorylation therefore provides a molecular marker for the activation state of Mek1. Analysis of T327 phosphorylation of Mek1 in various mutant conditions revealed several requirements for Mek1 activation in response to DSBs. In addition, MS identified a third amino acid in the activation loop, S320, which is also phosphorylated. Unlike that of T327 and T331, however, S320 phosphorylation is required specifically in maintaining Mek1 function in *dmc1*Δ-arrested cells.

TABLE 1. Plasmids

Name	Yeast genotype	Reference or source
pRS402	*ADE2*	7
pTS30	*GST-MEK1 ADE2*	9
pTS31	*GST-mek1-K199R ADE2*	9
pTS32	*GST-mek1-T327A ADE2*	45
pTS33	*GST-mek1-T327D ADE2*	45
pTS30-T331A	*GST-mek1-T331A ADE2*	This work
pTS30-T331D	*GST-mek1-T331D ADE2*	This work
pTS30-AA	*GST-mek1-T327A T331A ADE2*	This work
pTS30-AD	*GST-mek1-T327A T331D ADE2*	This work
pTS30-DA	*GST-mek1-T327D T331A ADE2*	This work
pTS30-DD	*GST-mek1-T327D T331D ADE2*	This work
pHN26	*GST-mek1-K199R URA3*	27
pHN31	*GST-mek1-T327A URA3*	This work
pHN32	*GST-mek1-T327D URA3*	This work
pHN33	*GST-mek1-T331A URA3*	This work
pHN34	*GST-mek1-T331D URA3*	This work
pHN35	*GST-mek1-T327D T331D URA3*	This work
pTS30-R51A	*GST-mek1-R51A ADE2*	45
pTS30-R72P D76K	*gst-R72P D76K-MEK1 ADE2*	27
pRS306	*URA3*	39
pBL12	*GST-MEK1 URA3*	27
pBL12-S320A	*GST-mek1-S320A URA3*	This work
pHN38	*gst-R72P D76K-mek1-S320A URA3*	This work
pLT11-K593A	*hop1-K593A URA3*	27
pSB3-K348E	*red1-K348E URA3*	47
pLP37	*MEK1 URA3*	9
pLP36	*mek1-K199R URA3*	9
pTS9	*mek1-T327A URA3*	This work
pTS15	*mek1-T327D URA3*	This work
pHN36	*mek1-T331A URA3*	This work
pHN37	*mek1-T331D URA3*	This work
pLP37-S142A	*mek1-S142A URA3*	This work
pLP37-S320A	*mek1-S320A URA3*	This work
pLP37-S142A S320A	*mek1-S142A S320A URA3*	This work
pLP37-S320D	*mek1-S320D URA3*	This work
pLP37-IL	*mek1-I459A L460A URA3*	This work
pEJ2	*GST-mek1-I459A L460A URA3*	This work
pEJ4	*gst-R72P D76K-mek1-I459A L460A URA3*	This work
pNH131	*rec104*Δ*::LEU2*	14
pHN30	*FKBP-MEK1 ADE2* 2μm	This work

MATERIALS AND METHODS

Plasmids. Plasmid names, genotypes, and sources can be found in Table 1. All *MEK1* alleles (including N-terminal fusions) are under control of the *MEK1* promoter. Mutations in T327 and T331 were introduced into *GST-MEK1* by site-directed mutagenesis of the *ADE2*-integrating plasmid pTS30 (QuikChange kit; Stratagene, La Jolla, CA). To create *URA3* integrating plasmids containing the P_{MEK1}-*GST-mek1* alleles (pHN31 to pHN35), 3.0-kb NotI/SalI fragments from the corresponding *ADE2* plasmids were subcloned into NotI/SalI-digested pRS306. Untagged *mek1* alleles (pTS9, pTS15, pHN36, and pHN37) were created by substituting 0.75-kb SpeI/HpaI fragments from *GST-mek1* mutant alleles for the corresponding fragment in pLP37. Mutations in S142 and S320 were made by site-directed mutagenesis in untagged and *GST*-tagged *MEK1* using pLP37 and pBL12 as templates, respectively. *mek1-I459A L460A* (*mek1-IL*) was created by introducing I459A and L460A into pLP37 to make pLP37-IL. A 0.5-kb HpaI/KpnI fragment from pLP37 was substituted for the analogous fragment in HpaI/KpnI-digested pBL12, thereby making *GST-mek1-IL* in pEJ2. For *gst-R72P D76K-mek1-IL*, a 2.6-kb HpaI/BamHI fragment from pTS30-R72P D76K replaced the analogous fragment in pEJ2 to make pEJ4. Mutations were confirmed by DNA sequencing (Stony Brook University DNA Sequencing Facility). All *mek1* alleles exhibiting a mutant phenotype were sequenced in their entirety to ensure that no unintended mutations were created during the mutagenesis. *gst-R72P D76K-mek1-S320A* was constructed by cloning a 1.9-kb SpeI fragment from pEJ4 containing *gst-R72P D76K* into SpeI-digested pBL12-S320A, thereby creating pHN38.

The *FKBP-MEK1* overexpression plasmid was constructed using plasmid pC_4-F_v1E from the ARGENT regulated homodimerization kit (ARIAD Pharmaceu-

TABLE 2. *S. cerevisiae* strains

Strain	Genotype	Reference or source
YTS1	*MAT***a** *leu2Δ hisG his4-x ARG4 ura3 lys2 hoΔ::LYS2 mek1Δ::LEU2* *MATα leu2-K HIS4 arg4-Nsp ura3 lys2 hoΔ::LYS2 mek1Δ::LEU2*	9
YTS1ade	Same as YTS1 but *ade2-Bgl*	9
NH520	*MAT***a** *leu2::hisG his4-x dmc1Δ::LEU2 hoΔ::LYS2 lys2 ura3 mek1Δ::kanMX6* *MATα leu2::hisG his4-B dmc1Δ::LEU2 hoΔ::LYS2 lys2 ura3 mek1Δ::kanMX6*	45
NH561	*MATα leu2-K HIS4 hoΔ::LYS2 lys2 ura3 arg4-Nsp mek1Δ::kanMX6 rec104Δ::LEU2* *MAT***a** *leu2ΔhisG his4-x hoΔLYS2 lys2 ura3 ARG4 mek1Δ::kanMX6 rec104Δ::LEU2*	This work
NH566	*MATα leu2 HIS4 lys2 hoΔ::LYS2 ura3 ade2 arg4 hop1::LEU2 mek1Δ::LEU2* *MAT***a** *leu2 his4 lys2 hoΔ::LYS2 ura3 ade2 arg4 hop1::LEU2 mek1Δ::LEU2*	27
NH423	*MAT***a** *leu2-k HIS4 hoΔ::LYS2 lys2 ura3 arg4-Nsp ade2-Bgl mek1Δ::LEU2 red1Δ::kanMX6* *MAT***a** *leu2Δ hisG his4-x hoΔ::LYS2 lys2 ura3 ARG4 ade2-Bgl mek1Δ::LEU2 red1Δ::kanMX6*	45

ticals) as a template to amplify *FKBP* by PCR. The fragment was engineered to introduce an NdeI site at the start codon of *FKBP* and EcoRI/SalI sites immediately downstream of the *FKBP* coding sequence. After digestion with NdeI and SalI, the PCR fragment was ligated to NdeI/SalI-digested pTS25 to fuse *FKBP* to the *MEK1* promoter and create pHN27. A BamHI/SalI fragment containing the P_{MEK1}-*FKBP* cassette was subcloned into BamHI/SalI-cut pRS402 to make pHN28. The *MEK1* coding sequence was fused in frame to *FKBP* by ligation of an EcoRI/SalI fragment from pTS3 into EcoRI/XhoI-digested pHN28, thereby creating pHN29. In this fusion the methionine of Mek1 is deleted and replaced with the amino acids FPGI. Finally, the P_{MEK1}-*FKBP-MEK1* fusion carried on a NotI/KpnI fragment was subcloned into NotI/KpnI-digested pRS422 to make pHN30.

Yeast strains and media. Strain genotypes are listed in Table 2. All strains are derived from SK1. The *mek1*Δ::*kanMX6 rec104*Δ::*LEU2* diploid, NH561, was constructed by transforming *mek1*Δ haploid strains S2683 *mek1*Δ::*KAN* and RKY1145 *mek1*Δ::*KAN* with BamHI/XbaI-digested pNH131. The presence of the *rec104*Δ::*LEU2* mutation was confirmed by Southern blot analysis and the haploids mated to make the diploid. All integrating plasmids were digested with StuI to target integration either to *ADE2* or *URA3* in diploid strains and are presumed to be present in single copy. Liquid and solid media were as described previously (9). Cultures were sporulated at a density of 3×10^7 cells/ml in 2% potassium acetate at 30°C. The ligand used to induce dimerization of human FK506 binding protein (FKBP), AP20187, was obtained from the ARGENT regulated homodimerization kit (ARIAD Pharmaceuticals).

Kinase assays and Western blots. For Western blots, GST-Mek1 was partially purified from 50 ml of cells after 4.5 h in sporulation medium (Spo medium) at 30°C as described previously (45). The precipitates were fractionated on 8% sodium dodecyl sulfate (SDS)-polyacrylamide gels, transferred to nitrocellulose membranes, and blocked with 5% nonfat milk for 1 h at room temperature. The blots were then incubated in 5% bovine serum albumin with a 1:1,000 dilution of Akt antibody (Cell Signaling Technology) and incubated at 4°C overnight. The blots were washed with TBS (20 mM Tris-HCl [pH 7.5], 250 mM NaCl, 0.1% Tween 20) and probed with anti-rabbit secondary antibodies (Bio-Rad) for 4 h before being developed using the Immun-Star horseradish peroxidase kit (Bio-Rad). To determine the relative amounts of GST-Mek1 in each pulldown, the blots were incubated in stripping buffer (50 mM Tris-HCl [pH 6.8], 2% SDS, 50 mM dithiothreitol [DTT]) at 55°C for 30 min and then probed with a 1:5,000 dilution of anti-GST antibodies (generously provided by Doug Kellogg, University of California, Santa Cruz). Kinase assays using glutathione-precipitated GST-Mek1 were performed as described previously (26) except that 0.2 mM ATP without any radioactivity was used.

Protein purification and MS. For MS analysis, GST-Mek1 was purified from the *GST-MEK1 dmc1*Δ diploid, NH520::pBL12. One liter of sporulating culture (~10 g of cell pellet) was collected 5 h after transfer to Spo medium at 30°C. Soluble extracts were made by resuspending the cells in 10 ml lysis buffer (50 mM Tris [pH 8.0], 10 mM EDTA 8.0, 300 mM NaCl, 1 mM DTT, 0.5% Triton X-100, 0.05% SDS, 1 mM phenylmethylsulfonyl fluoride, 1 μg/ml leupeptin, 1 μg/ml aprotinin, 1 μg/ml pepstatin, 2 mM benzamidine, 10 mM NaF, 1 mM $Na_4P_2O_7$) and 10 g acid-washed glass beads and vortexing for 20 seconds 10 times, with 2 min on ice in between. Five hundred microliters of glutathione-Sepharose (GE Health Science) was added and incubated at 4°C with rotation for 2 h. GST-Mek1 was eluted by the addition of 500 μl elution buffer (50 mM Tris-HCl [pH 7.5], 200 mM NaCl, 1 mM DTT, 10 mM glutathione). The flowthrough was collected, and this step was repeated twice. All three flowthroughs were pooled, and GST-Mek1 was precipitated by addition of trichloroacetic acid to a final concentration of 20% and then incubated on ice for 20 min. The precipitate was collected by centrifugation at 16,000 × *g* for 20 min at 4°C. The pellet was washed with 100% acetone and the protein fractionated using a 4 to 12% bis-Tris NuPAGE gel (Invitrogen).

Proteins were stained in the gel using Gel-code Blue reagent (Pierce), and the GST-Mek1 band was cut out of the gel. The band was cut into approximately 1-mm cubes, washed with MilliQ water, and destained using 50% CH_3CN–50 mM NH_4HCO_3. Gel pieces were dehydrated with 100% CH_3CN and dried for 30 min under vacuum. For in-gel digestion, dry gel pieces were rehydrated with 10 ng/μl trypsin (50 mM NH_4HCO_3, pH 8) on ice for 2 h. The digestion was carried out at 37°C overnight. Digests were extracted twice using a solution of 50% CH_3CN–5% HCOOH, dried completely under vacuum, and stored at −80°C until further analysis.

Liquid chromatography-tandem MS experiments were performed on an LTQ mass spectrometer (Thermo Electron, San Jose, CA). Peptide mixtures were loaded onto a 100-μm-inner-diameter fused-silica microcapillary column packed in-house with C_{18} resin (Michrom Bioresources Inc., Auburn, CA) and were separated using a 40-min gradient from 8% to 45% solvent B (0.15% HCOOH–97.5% CH_3CN). Solvent A was 0.15% HCOOH–2.5% CH_3CN. The LTQ mass spectrometer was operated in the data-dependent mode using the TOP10 strategy (11, 23). In brief, a scan cycle was initiated with a full scan, which was followed by tandem MS scans on the 10 most abundant precursor ions with dynamic exclusion of previously selected ions.

Time courses. Liquid sporulation was performed at 30°C with 2% potassium acetate. Sporulation was monitored using phase-contrast light microscopy to count the number of asci present in 200 cells per strain. Meiotic progression was monitored by staining cells with DAPI (4′,6′-diamidino-2-phenylindole) using fluorescence microscopy. Binucleate cells have completed MI, while tetranucleate cells have completed MII. DSBs were monitored at the naturally occurring YCR048w hot spot as described previously (47, 48). DSBs were quantitated using a Molecular Dynamics PhosphorImager (Amersham, Piscataway, NJ) and Image Quant 1.1 software.

RESULTS

Two conserved threonines in the Mek1 activation domain are important for Mek1 function. Alignment of budding yeast Mek1 with different kinases activated by phosphorylation as well as different fungal orthologs of Mek1 indicates that there are two conserved threonine residues within Mek1's activation domain, T327 and T331 (Fig. 1A). Although genetic evidence exists for a role of T327 in Mek1 function, a role for T331 has not been reported (45). Various T327/T331 mutant combinations were therefore introduced by site-directed mutagenesis into *GST-MEK1*, and the mutants were tested for complementation of the *mek1*Δ spore viability defect. As was previously observed, mutation of T327 to alanine reduces spore viability, while the presence of a negatively charged amino acid at this position (*GST-mek1-T327D*) creates a more functional allele (45) (Table 3). Alteration of T331 to alanine decreased spore viability sig-

A

```
                320      327  331
Scer:  DFGIAKDLNSN-KERMHTVVGTPEYCAPEV
Klac:  DFGIAKELSQNTKERMHTVVGTPEYCAPEV
Agos:  DFGIAKDLPST-RVRMHTIVGTPEYCAPEV
Cagl:  DFGIAR-TVTTMKSRMFTVVGTPEYCAPEV
Spmb:  DFGVAR--CMQKGKRLSTFVGTPEYTAPEI
CaMKI: DFGLSK--MEDPGSVLSTACGTPGYVAPEV
PKA:   DFGFAK--RVK-G-RTWTLAGTPEYLAPEI
```

B

Phosphorylation sites	Peptide	*m/z*	Charge State	Xcorr[a]
Thr_{327}	$M^{ox}HT\#VVGTPEYCAPEVGFR$	716.5	3	4.2
Thr_{331}	$M^{ox}HTVVGT\#PEYCAPEVGFR$	716.5	3	5.0
Thr_{327}, Thr_{331}	MHT#VVGT#PEYCAPEVGFR	737.8	3	2.2

[a]XCorr values were from the Sequest algorithm
M^{ox}: Met is oxidized

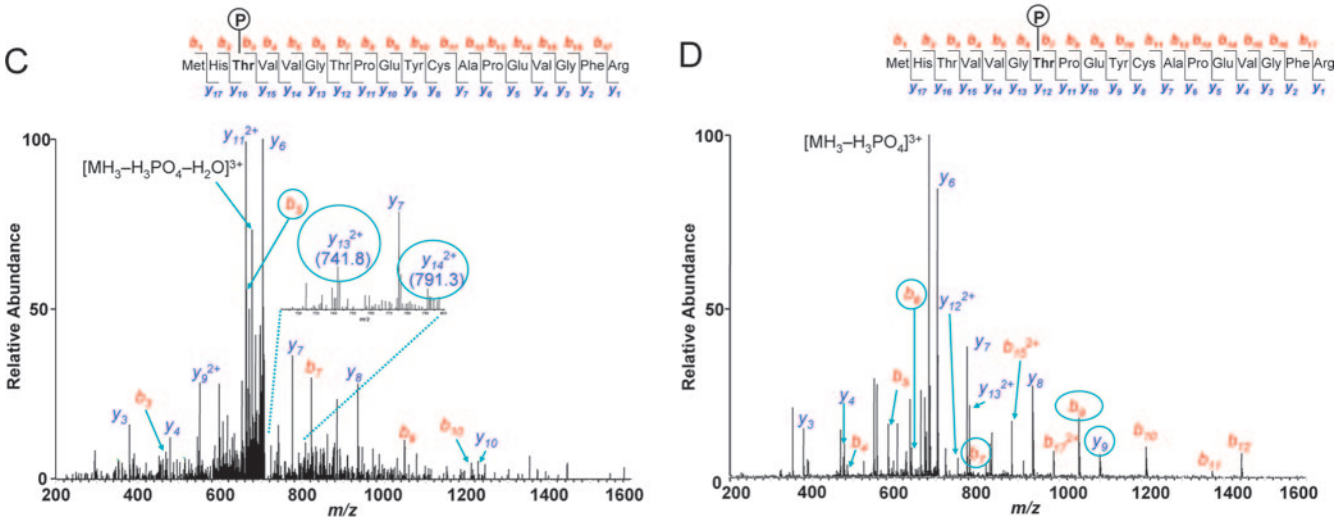

FIG. 1. MS analysis of phosphorylated threonines in the Mek1 activation domain. (A) Alignment of activation domains of Mek1 proteins from different fungal species and from mammalian CaMKI and PKA. Bold letters indicate conserved threonines. Numbers indicate amino acid position in *S. cerevisiae* Mek1. Scer, *S. cerevisiae*; Scas, *Saccharomyces castellii*; Agos, *Ashbya gossypii*; Klac, *Kluyveromyces lactis*; Cagl, *Candida gilbrata*; Spmb, *S. pombe*; CaMKI, calcium/calmodulin-dependent protein kinase I (from rat); PKA, cAMP-dependent protein kinase (from mouse). (B). Summary of peptides detected as phosphorylated at T327 and/or T331. T#, phosphorylated threonine. (C and D) Tandem MS of monophosphorylated phosphopeptides, showing site localization to either T327 (C) or T331 (D). These two phosphopeptides had different retention times, and their fragmentation spectra were also different. Fragment ions used to determine site localization are circled. Cysteine residues were found as carboxyamidomethylated products, and methionines were found in their oxidized state.

nificantly to 20.1%, indicating that T331 is also required for Mek1 to function properly during meiosis. In this case, however, the presence of a phosphomimetic amino acid at this position did not improve the phenotype, producing only 12.9% viable spores (Table 3). This result could mean either that T331 is not normally phosphorylated or, more likely, that aspartic acid is not a good mimic for phosphate at this position.

The ability of the activation loop mutants to mediate *dmc1*Δ arrest was also analyzed. The *dmc1*Δ *GST-mek1-T327A* and *dmc1*Δ *GST-mek1-T327D* mutants both sporulated as well as the *dmc1*Δ *GST-mek1-K199R* mutant (with a catalytically inactive version of Mek1) (Table 3). DSBs are repaired in these diploids, and the spores are inviable (data not shown), indicating that these mutants are defective in the BSCR. These results suggest that *dmc1*Δ arrest requires a higher level of kinase activity than what is required for creating a BSCR in an otherwise wild-type meiosis. This could be because the BSCR functions only transiently in a *DMC1* diploid, whereas it must function constitutively in *dmc1*Δ-arrested cells to prevent repair off sister chromatids and, consequently, meiotic progression and sporulation.

The untagged *mek1-T327D* mutant exhibits higher spore viability than the *mek1-T327A* mutant, although the absolute number of viable spores is much lower than with *GST-mek1* mutants (Table 3). One explanation is that binding of predimerized GST-Mek1 to phospho-Red1 results in a higher local concentration of the kinase than for untagged Mek1 (bringing two kinase molecules to Red1 instead of one). Consistent with the low level of activity in the untagged activation domain mutants, no *dmc1*Δ arrest was observed (Table 3).

Examination of various double mutant combinations suggests that phosphorylation of T327 and/or T331 occur during meiosis. Although neither the T327A nor the T331A single mutant decreases spore viability to the null level, the *mek1-T327A T331A* mutant produced 6.5% viable spores, equivalent to the catalytically inactive *mek1-K199R* mutant (Table 3) (9). Therefore, some functional redundancy exists between these two sites. If the presence of a negative charge at T327 is sufficient for Mek1 kinase activation, then aspartic acid at this position should bypass the requirement for phosphorylation at T331. However, this is not the case, as the *mek1-T327D T331A* mutant resembles the *mek1-T331A* mutant and not the *mek1-T327D* mutant (Table 3). Therefore, the function of T331 phosphorylation is not simply to promote phosphorylation of T327. The *mek1-T327D T331D* mutant generates significantly more viable spores than either the *mek1-T327D T331A* or *mek1-T327A T331D* mutant, as well as exhibiting partial

TABLE 3. Spore viability of mutants with various mutations in the Mek1 activation loop

MEK1 genotype[a]	% Spore viability (no. of asci)[b]	% Sporulation (mean ± SD) in *dmc1*Δ background[c]
*mek1*Δ	6.8 (108)	70.7 ± 8.6
GST-mek1-K199R	7.4 (91)	ND[d]
GST-MEK1	87.8 (39)***	0 ± 0
GST-mek1-T327A	35.5 (105)***	69.2 ± 16.3
GST-mek1-T327D	73.3 (104)***	72.2 ± 15.8
GST-mek1-T331A	20.1 (108)***	71.8 ± 16.4
GST-mek1-T331D	12.9 (101)*	73.7 ± 12.4
GST-mek1-T327A T331A	6.5 (106)	ND
GST-mek1-T327D T331A	6.8 (96)	ND
GST-mek1-T327A T331D	6.6 (102)	ND
GST-mek1-T327D T331D	15.4 (117)**	51.3 ± 11.5
MEK1	96.2 (26)***	1.3 ± 1.1
mek1-K199R	<1.0 (26)	65.5 ± 0.5
mek1-T327A	<0.3 (104)	80.0 ± 4.3
mek1-T327D	4.3 (104)***	80.3 ± 4.6
mek1-T331A	2.9 (104)**	81.0 ± 0.5
mek1-T331D	2.4 (104)	71.3 ± 6.4

[a] For spore viability of *GST-mek1* mutants, *ADE2* plasmids were integrated into YTS1ade. For untagged *mek1* alleles, *URA3* plasmids were integrated into YTS1. For analysis of *dmc1*Δ arrest, *URA3 GST-mek1* and *URA3 mek1* plasmids were integrated into NH520.

[b] To assess spore viability, transformants were patched onto minimal medium lacking either adenine or uracil, replicated to Spo plates, incubated at 30° for 24 h, and then dissected. Asterisks indicate spore viability values that are statistically significantly increased compared to those for *mek1*Δ based on χ^2-analysis: *, $P < 0.01$; **, $P < 0.001$; ***, $P < 0.0001$. χ^2 analysis was performed using software present at http://faculty.vassar.edu/lowry/tab2X2.html. For *mek1-T331D*, there were insufficient data to perform the χ^2 analysis.

[c] To monitor sporulation, transformants were patched onto SD-uracil plates and replica plated to Spo medium for 24 h at 30°C, and 200 cells were assayed for formation of asci by phase-contrast light microscopy. Three transformants were analyzed for each plasmid.

[d] ND, no data.

*dmc1*Δ arrest, suggesting that negative charges at both positions promote Mek1 activation (Table 3).

Mek1 is phosphorylated on T327 and T331 in meiotic cells. To obtain direct biochemical evidence that T327 and/or T331 is phosphorylated on Mek1 during meiosis, MS was used to map phosphorylation sites on GST-Mek1 purified after 5 h in Spo medium. A *dmc1*Δ diploid was used because Mek1 is constitutively active during *dmc1*Δ arrest to prevent *DMC1*-independent repair of DSBs (45). Therefore *dmc1*Δ provides a way of synchronizing meiotic cells at a time after Mek1 has been activated. After glutathione-Sepharose precipitation and elution, GST-Mek1 was fractionated by SDS-polyacrylamide gel electrophoresis and the protein cut out of the gel and digested with trypsin. The Mek1 peptides were subjected to phosphorylation analysis by liquid chromatography-tandem MS techniques (32). Phosphopeptides were identified by database searching using the Sequest algorithm. A doubly phosphorylated peptide with the sequence MHT*VVGT*PEYCS PEVGFR was identified. The phosphorylated threonines in this peptide are T327 and T331, respectively. Both monophosphorylated forms of the peptide were also found (Fig. 1B). Tandem mass spectra for each event are shown in Fig. 1C and D. Combining the genetic and biochemical data, these experiments demonstrate that phosphorylation of the Mek1 activation domain is essential for accurate chromosome segregation during meiosis.

Phosphorylation of T327 is dependent upon DSBs and Hop1/Red1/Mek1 complexes. T327 is contained within the peptide KXRXXT, which, after being phosphorylated, matches the recognition site of the commercially available phospho-(Ser/Thr) Akt substrate antibody (25). GST-Mek1 was partially purified from meiotic cells and probed on immunoblots with the Akt antibodies. A strong signal was detected from the strain carrying *GST-MEK1* but not from the *mek1*Δ strain (Fig. 2). The blot was stripped and then reprobed with anti-GST antibodies to confirm that the protein being analyzed was GST-Mek1 (Fig. 2). No signal was detected for either GST-*mek1-T327D* or GST-*mek1-T327A*, indicating that the antibody was specifically recognizing phosphorylation at T327 (Fig. 2 and data not shown). The Akt antibodies therefore provide a means of probing the activation state of Mek1 in vivo under various mutant conditions.

REC104 encodes a meiosis-specific protein that is required to generate DSBs (30). No phospho-T327 was detected in GST-Mek1 partially purified from a *rec104*Δ diploid after 4.5 h in Spo medium (Fig. 2). (In strains that reduce or abolish T327 phosphorylation, a faint band that migrates slightly faster than GST-Mek1 is sometimes observed [Fig. 2]. However, because this band is not reproducibly observed in other experiments, it is unlikely to be phosphorylated GST-Mek1 [data not shown].) The failure of GST-Mek1 to be phosphorylated at T327 in *rec104*Δ diploids indicates that DSBs are required for Mek1 activation.

Hop1/Red1/Mek1 complexes can be disrupted by a variety of mutations. Deletion of either *HOP1* or *RED1* destroys the complex, and GST-Mek1 fails to undergo T327 phosphorylation in both cases (Fig. 2). In addition there are mutants that interfere with specific parts of the complex. For example, *GST-mek1-R51A* contains a point mutation in the Mek1 FHA domain that specifically disrupts the interaction of Mek1 with phospho-Red1 (45). This mutation prevents T327 phosphorylation, indicating that Mek1 cannot be activated unless it is

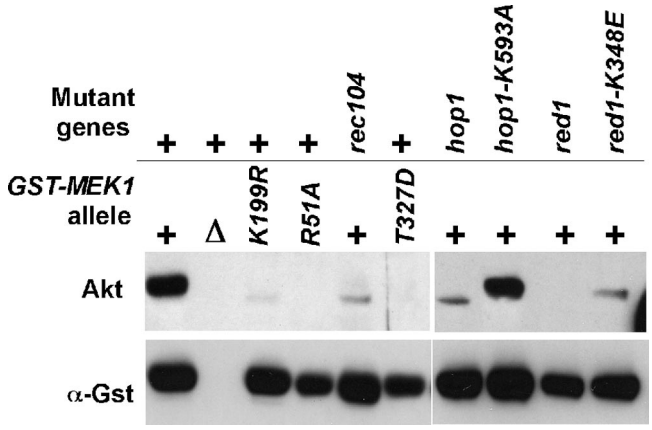

FIG. 2. Mek1 T327 phosphorylation under different mutant conditions. GST-Mek1 was partially purified from the indicated diploids after 4.5 h in Spo medium at 30°C. *GST-MEK1* (YTS1ade::pTS30), *mek1*Δ (YTS1ade::pRS402), *GST-mek1-K199R* (YTS1ade::pTS31), *GST-mek1-R51A* (YTS1ade::pTS30-R51A), *GST-mek1-T327D* (YTS1ade::pTS33), *GST-MEK1 rec104*Δ (NH561::pBL12), *GST-MEK1 hop1*Δ (NH566::pRS306::pTS30), *GST-MEK1 hop1-K593A* (NH566::pLT11-K593A::pTS30), *GST-MEK1 red1*Δ (NH423::pTS30::pRS306), and *GST-MEK1 red1-K348E* (NH423::pTS30::pSB3-K348E) mutants were used. Proteins were fractionated by SDS-polyacrylamide gel electrophoresis and probed with Akt antibodies to detect T327 phosphorylation. The blot was then stripped and reprobed with anti-GST antibodies to detect total Mek1 protein.

bound to Red1 (Fig. 2). The *red1-K348E* mutant is specifically defective for interaction with Hop1, and this mutant exhibits a reduced amount of phospho-T327 (47) (Fig. 2). Finally, T327 is phosphorylated in *GST-MEK1*::*hop1-K593A* diploids, where the Hop1 C domain requirement for Mek1 dimerization has been bypassed by GST, while other functions remain intact (Fig. 2).

T327 phosphorylation requires Mek1 kinase activity. No in vivo T327 phosphorylation is observed when Mek1 is catalytically inactive (*GST-mek1-K199R*), indicating that Mek1 activates itself by autophosphorylation (Fig. 2). Further evidence for this idea comes from the finding that GST-Mek1 can phosphorylate T327 in vitro. To show this, GST-Mek1 lacking in vivo T327 phosphorylation was first purified from *hop1*Δ and *rec104*Δ diploids. The beads containing the precipitated kinase were then split into two tubes containing kinase assay buffer. ATP was added to one tube, and the proteins were incubated at 30°C for 30 min. The kinase incubated without ATP exhibits the in vivo phosphorylation state of Mek1, whereas the presence of ATP allows Mek1 phosphorylation to occur in vitro. GST-Mek1 from the wild type is phosphorylated in vivo on T327, but the Akt signal is increased after incubation with ATP, suggesting that additional phosphorylation of T327 is occurring in vitro (Fig. 3). This idea was confirmed by observing that T327 is phosphorylated in the kinase purified from the *hop1*Δ and *rec104*Δ diploids only after incubation with ATP (Fig. 3). No T327 phosphorylation was observed with GST-Mek1-K199R with or without ATP, demonstrating that both in vivo and in vitro T327 phosphorylations require Mek1 kinase activity and are not due to a copurifying kinase. These results suggest that Mek1 activates itself by autophosphorylation of T327.

The Akt antibodies were used to directly examine whether phosphorylation of T331 is required for T327 phosphorylation. GST-Mek1-T331A exhibited autophosphorylation of T327 in vitro, although the amount of phosphorylated kinase was less than that observed with GST-Mek1-T331D, which, in turn, was less than that with GST-Mek1 (Fig. 3B). Therefore it appears that a negative charge at T331 enhances the ability of Mek1 to phosphorylate itself at T327 but is not absolutely required.

***MEK1* function in *hop1-K593A* mutants is dependent upon dimerization.** A variety of correlative data from genetic experiments indicate that Mek1 dimerization mediated by the Hop1 C domain is important for kinase function. However, biochemical experiments to detect Mek1 dimers by coimmunoprecipitation have thus far been unsuccessful. To confirm that dimerization is the critical function conferred by GST when *GST-MEK1* suppresses *hop1-K593A*, a version of *MEK1* in which dimerization can be regulated was created. Addition of the human FKBP to a protein enables conditional dimerization by addition of a ligand containing two FK506 moieties (AP20187) to the medium (see, e.g., reference 46). Overexpression of *FKBP-MEK1* partially complements *mek1*Δ in either the absence or presence of ligand (76% and 70% viable spores, respectively), indicating that FKBP does not interfere with Hop1 C-domain-promoted dimerization of Mek1. However, in the *hop1-K593A* background, *FKBP-MEK1* produced only 2% viable spores (65 tetrads) in the undimerized form. Addition of AP20187 to the culture increased spore viability to 40% (87 tetrads), demonstrating that dimerization of Mek1 enhances kinase function under these conditions.

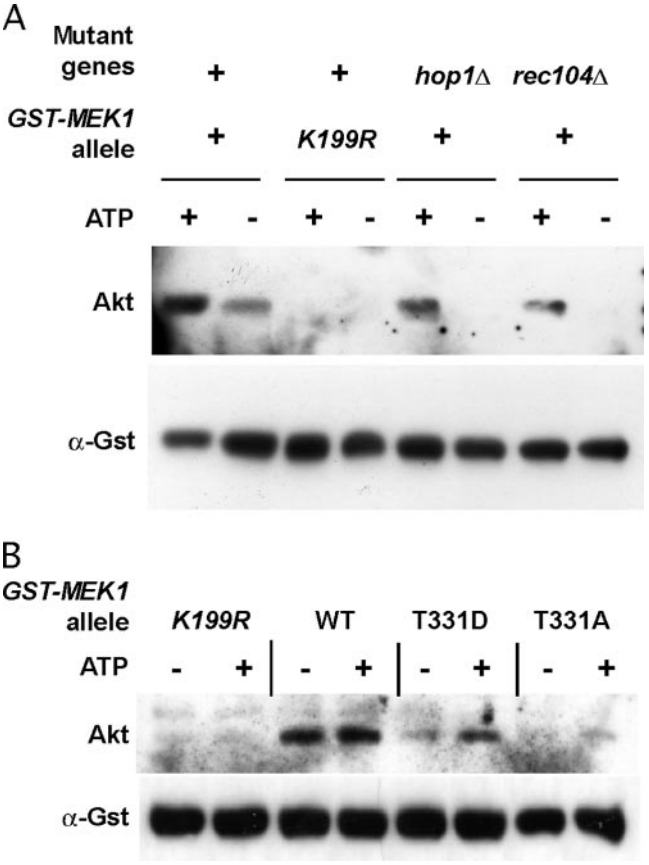

FIG. 3. Comparison between in vivo and in vitro T327 phosphorylation of GST-Mek1 under different mutant conditions. (A) GST-Mek1 was partially purified from wild-type (YTS1ade::pTS30), *hop1*Δ (NH566::pRS306::pTS30), or *rec104* (NH561::pBL12) diploids sporulated for 4.5 h at 30°C. As a control, GST-Mek1-K199R was purified from a wild-type strain (YTS1ade::pTS31) under the same conditions. The beads containing the precipitated kinase were washed, split in half, and resuspended in kinase assay buffer at 30°C for 30 min in the presence (+) or absence (−) of ATP. Phosphorylated T327 and total GST-Mek1 were detected as described in the legend to Fig. 2. (B) GST-Mek1 was partially purified from the wild type (YTS1::pBL12) and from *GST-mek1-K199R* (YTS1::pHN26), *GST-mek1-T331D* (YTS1::pHN34), and *GST-mek1-T331A* (YTS1::pHN33) mutants and processed as described for panel A.

The Mek1 C terminus contains a putative homodimerization domain. The Mek1 protein can be divided into three distinct domains: an FHA domain in the N terminus, a catalytic domain in the middle of the protein, and a functionally uncharacterized 50-amino-acid C-terminal tail (pfam domain analysis; http://www.sanger.ac.uk/Software/Pfam/) (Fig. 4A). Alignment of the C-terminal domains of Mek1 proteins from different fungal species reveals a conserved sequence of approximately 20 amino acids located immediately downstream of the catalytic domain (Fig. 4B). If this region allows *HOP1*-mediated dimerization of Mek1, then mutation of conserved amino acids within this domain should disrupt Mek1 function, and these defects should be suppressed by ectopic dimerization of Mek1 by GST. Replacement of two conserved amino acids within the Mek1 C-terminal tail with alanine (*mek1-I459A*

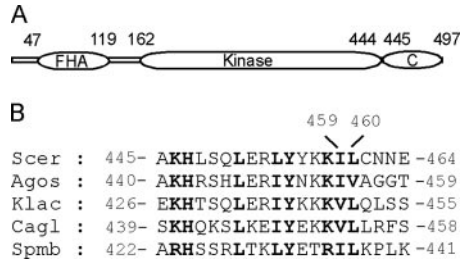

FIG. 4. Functional domains of Mek1. (A) Diagram indicating the positions of the FHA, catalytic, and C-terminal domains. (B) Alignment of the sequences of the C-terminal tails of Mek1 proteins from different fungal species. Bold letters indicate conserved residues. I459 L460 are indicated.

L460A [*mek1-IL*]) creates an allele of *MEK1* that is nearly null for both spore viability and *dmc1*Δ arrest (Table 4; Fig. 5A). Furthermore, the *mek1-IL* mutant is defective in the BSCR, as evidenced by the repair of DSBs in the *dmc1*Δ background (Fig. 5B and C). The IL mutations do not interfere with the catalytic activity of Mek1, as the spore viability and *dmc1*Δ arrest defects of the *mek1-IL* mutant are suppressed if the allele is fused to *GST* (Table 4; Fig. 5A). DSBs are unrepaired in *dmc1*Δ *GST-mek1-IL* diploids, indicating that the BSCR has been restored (Fig. 5B and C). Ectopic dimerization mediated by GST is required for suppression of the *mek1-IL* mutant. Mutations in *GST* that disrupt dimerization (*gst-RD-mek1-IL*) abolish suppression of *mek1-IL*, producing inviable spores and failing to arrest in the *dmc1*Δ background (27) (Table 4). Direct proof that this region of Mek1 confers dimerization awaits the development of a biochemical assay that can detect Mek1 oligomers.

Phosphorylation of an amino acid within the Mek1 activation domain is required to maintain *MEK1* function in *dmc1*Δ-arrested cells. MS of GST-Mek1 not only confirmed that T327 and T331 are phosphorylated in vivo but also revealed two previously unknown phosphorylation sites: serine 142 and serine 320. S142 is located between the FHA and catalytic domains of Mek1, while S320 resides within the activation loop (Fig. 1 and 4). These serines were mutated in *MEK1* both individually (*mek1-S142A* and *mek1-S320A*) and in combination (*mek1-S142A S320A*) and tested for their ability to complement the spore inviability of the *mek1*Δ mutant. All three mutant alleles complemented nearly as well as *MEK1*, producing ≥93% viable spores, indicating that phosphorylation of these amino acids does not play a critical role in wild-type meiosis (Table 5). Given that the GST-Mek1 protein used for MS was purified from a *dmc1*Δ mutant, one possibility is that phosphorylation of S142 and/or S320 is specifically required in *dmc1*Δ-arrested cells. Therefore the ability of the three mutants to maintain *dmc1*Δ arrest was also examined. The *mek1-S142A* mutant behaves like the wild type in that it fails to sporulate in the *dmc1*Δ background (Table 5). The failure to identify a phenotype for the S142A mutation makes the functional significance of this phosphorylation unclear. In contrast, *mek1-S320A* and *mek1-S142A S320A* are partially defective in *dmc1*Δ arrest, allowing 58% and 56% sporulation, respectively (Table 5). Meiotic progression in the *mek1-S320A dmc1*Δ diploid is nearly as efficient as that in the catalytically inactive *mek1-K199R dmc1*Δ diploid (Fig. 6A). Mimicking the phosphorylated state by replacement of S320 with aspartic acid restores Mek1 function, as a *mek1-S320D dmc1*Δ mutant exhibits prophase arrest and only 4% sporulation (Table 5; Fig. 6A). These experiments demonstrate that phosphorylation of S320 is important for Mek1 function specifically during *dmc1*Δ arrest.

To see what effect S320 phosphorylation has on intersister DSB repair, DSBs at the *YCR048w* recombination hot spot were monitored in *dmc1*Δ, *mek1-K199R dmc1*Δ and *mek1-S320A dmc1*Δ diploids up to 12 h after transfer to Spo medium. As expected, DSBs were hyperresected and unrepaired in the *dmc1*Δ diploid and the cells arrested in prophase (Fig. 6). In contrast, DSBs were rapidly repaired in the *mek1-K199R dmc1*Δ and *mek1-S320A dmc1*Δ diploids (Fig. 6C). Replacement of S320 with aspartic acid prevented *DMC1*-independent DSB repair (Fig. 6B and C), indicating that a negative charge at this position is sufficient for Mek1 function. Because S320A has no phenotype in otherwise wild-type diploids, S320 phosphorylation appears to be required only to keep Mek1 functional and the BSCR active when resected DSBs are unable to invade homologous chromosomes.

Ectopic dimerization suppresses *mek1-S320A*. Fusion of *GST* to *mek1-S320A* restores *MEK1* function, reducing sporulation in the *dmc1*Δ background (Table 5). Preventing GST dimerization eliminates this suppression: the *gst-RD-mek1-S320A* mutant exhibits 64% sporulation in the *dmc1*Δ background and the spores are inviable, as expected if repair is occurring using sister chromatids as templates. Therefore, one possible function for S320 phosphorylation is to stabilize Mek1 dimers when cells are arrested by the meiotic recombination checkpoint.

DISCUSSION

Mek1 function requires phosphorylation of conserved threonines in the Mek1 activation loop. Phosphorylation of specific conserved amino acids within the activation loops of protein kinases such as protein kinase A (PKA) and insulin receptor kinase (IRK) plays a crucial role in kinase activation. PKA and IRK are members of the RD family of protein ki-

TABLE 4. Spore viability and *dmc1*Δ arrest phenotypes of *mek1-IL* in the presence or absence of GST

MEK1 genotype[a]	% Spore viability (no. of asci)	% Sporulation (mean ± SD) in *dmc1*Δ background[b]
MEK1	97.9 (48)	1.8 ± 1.7
GST-MEK1	94.5 (50)	0.7 ± 0.8
*mek1*Δ	1.1 (44)	95.9 ± 2.3
mek1-IL	4.4 (120)	82.5 ± 11.6
GST-mek1-IL	67.2 (122)	1.6 ± 0.8
gst-RD-mek1-IL	2.1 (24)	88.4 ± 2.2

[a] Plasmids containing the indicated *MEK1* alleles were integrated either into YTS1 (*mek1*Δ) to measure spore viability or into NH520 (*mek1*Δ *dmc1*Δ) to measure *dmc1*Δ arrest. *gst-RD* contains the R72P D76K mutations in GST that disrupt dimerization.

[b] Four independent transformants were transferred to Spo plates and incubated at 30°C for at least 24 h. Formation of asci was measured for 200 cells/transformant by phase-contrast light microscopy.

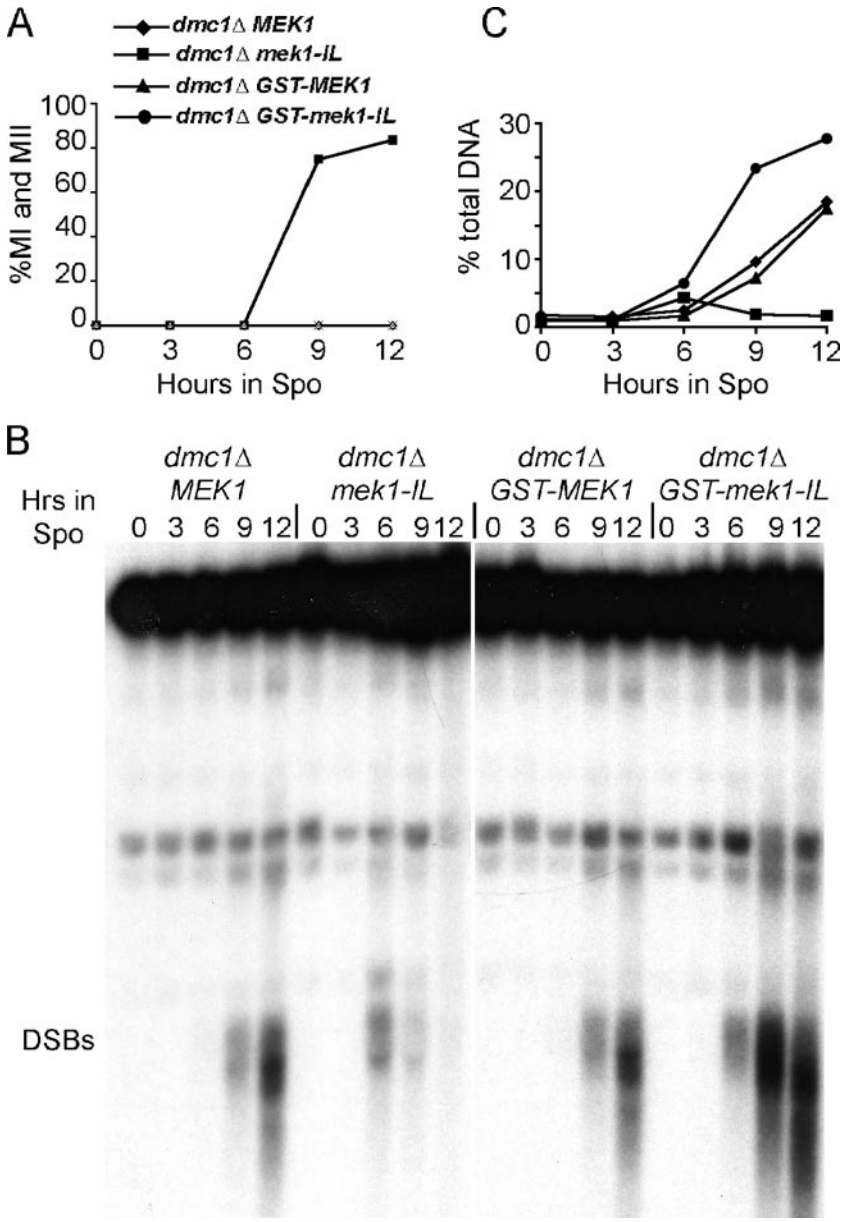

FIG. 5. Meiotic time course analysis of *mek1-IL dmc1*Δ and *GST-mek1-IL dmc1*Δ mutants. *MEK1 dmc1*Δ (NH520::pLP37), *mek1-IL dmc1*Δ (NH520::pLP37-IL), *GST-MEK1 dmc1*Δ (NH520::pBL12), and *GST-mek1-IL dmc1*Δ (NH520::pEJ2) mutants were transferred to Spo medium at 30°C, and samples were taken at 3-h intervals. (A) Meiotic progression measured by DAPI staining of cells to determine the fractions of binucleate (MI) and tetranucleate (MII) cells. Two hundred cells were counted for each strain at each time point. (B) DSBs detected at the *YCR048w* hot spot on chromosome III. (C) Quantitation of the DSB gel shown in panel B.

nases, in that they contain an arginine immediately upstream of an invariant catalytic aspartic acid residue within the kinase domain (18). Structural studies of active and inactive forms of PKA and IRK have shown that phosphorylation of the activation loop can promote conformational changes that allow proper substrate recognition as well as facilitating the phosphoryl transfer step (17, 18). Although in many cases, phosphorylation of a single amino acid within the activation loop is sufficient, there are examples where two to three phospho residues are required for maximum kinase activity (22, 34).

Mek1 is a member of the RD kinase family. Alignment of the Mek1 activation domain sequences with those of other RD protein kinases identified two conserved threonines, T327 and T331. Phosphorylation of the equivalent threonines in many kinases is required for activation. Mutations in *MEK1* that prevent phosphorylation of T327 and/or T331 reduce spore viability, abolish *dmc1*Δ arrest, and allow DSB repair in *dmc1*Δ diploids, indicating that these amino acids are functionally important during meiosis. Substitution of phosphomimetic amino acids for T327 and T331 partially complements a *mek1*Δ mutant, providing further support that the negative charge conferred by phosphorylation at these positions is important for kinase activation. MS analysis confirmed that T327 and T331 are phosphorylated in vivo. We conclude that Mek1 ki-

TABLE 5. Spore viability and *dmc1*Δ arrest phenotypes of additional Mek1 phosphorylation site mutants

MEK1 genotype[a]	*DMC1* background		*dmc1*Δ background	
	% Spore viability (no. of asci)	% Sporulation (mean ± SD)[b]	% Spore viability (no. of asci)	% Sporulation (mean ± SD)
MEK1	100.0 (13)	87.2 ± 2.6	ND[c]	0.0 ± 0.0
mek1-K199R	<2.0 (13)	89.8 ± 1.8	<2.0 (13)	81.7 ± 6.3
mek1-S142A	100.0 (13)	88.8 ± 0.3	ND	0.5 ± 0.5
mek1-S320A	93.6 (39)	85.7 ± 5.5	3.9 (26)	58.0 ± 5.3
mek1-S142A S320A	95.2 (79)	88.2 ± 2.0	2.0 (13)	56.3 ± 4.7
mek1-S320D	94.9 (39)	76.0 ± 11.9	ND	4.1 ± 3.2
GST-mek1-S320A	100.0 (13)	86.5 ± 2.6	ND	1.3 ± 1.4
gst-RD-mek1-S320A	89.4 (26)	82.2 ± 8.4	4.8 (26)	63.7 ± 5.3

[a] Plasmids containing the indicated *MEK1* allele were integrated into either YTS1 (*mek1*Δ) or NH520 (*mek1*Δ *dmc1*Δ). *gst-RD* contains the R72P D76K mutations in GST that disrupt dimerization (27).
[b] Sporulation was measured by counting the number of asci present in 200 cells/transformant using phase-contrast light microscopy. Three independent transformants were measured for all the alleles except *mek1-S320D*, where six transformants were analyzed for each strain.
[c] ND, no data.

nase activity is positively regulated by phosphorylation of the activation domain during meiosis.

Mek1 activation occurs by autophosphorylation. Mek1 kinase activity is required to suppress Rad51-mediated DSB repair between sister chromatids during meiosis, thereby promoting recombination between homologs (27, 45). This suppression is necessary only where DSBs are created, when the choice of whether to invade the sister chromatid or the homolog must be made. Because Mek1 kinase activity is required constitutively after DSB formation to prevent *DMC1*-independent repair, creation of a BSCR could be regulated at the level of Mek1 kinase activation. Hop1 is a DSB-dependent phosphoprotein, and the C domain of Hop1 promotes Mek1 dimerization (27). Therefore, DSB formation and Mek1 kinase activation could be coupled by Hop1-induced dimerization of Mek1, where dimerization enables kinase activation by phosphorylation of T327/T331 in *trans*. Attempts to test this idea using in vitro Mek1 autophosphorylation as the assay for kinase activation have been unsuccessful, however, in that mutants predicted to prevent kinase activation such as *rec104*Δ or *hop1*Δ mutants, exhibit little to no reduction in GST-Mek1 kinase activity compared to the wild type (reference 45 and data not shown). The Akt antibodies specifically detect phosphorylated T327 and therefore provide an alternative method for monitoring Mek1 kinase activation. Use of these antibodies revealed that Mek1 is able to phosphorylate itself on the activation loop during in vitro kinase reactions. The high levels of in vitro kinase activity observed for GST-Mek1 purified from mutant strains can therefore be attributed, at least in part, to activation of the kinase in the test tube after being isolated from the cell extract. GST-Mek1 with alanine substitutions at both T327 and T331 exhibits ~60% of the kinase activity of wild-type GST-Mek1 in vitro (C. Park and N. M. Hollingsworth, unpublished results). This result suggests that the unactivated enzyme has some basal activity which may allow significant levels of autophosphorylation when concentrated by the GST pulldown. Furthermore, at least in vitro, Mek1 is able to phosphorylate amino acids other than T327 and T331. For Mek1, therefore, in vitro kinase assays measuring autophosphorylation are not a good measure of kinase activation in vivo. The Akt antibodies circumvent this problem. The fact that both in vivo and in vitro T327 phosphorylation requires Mek1 catalytic activity indicates that Mek1 kinase activation is due to autophosphorylation.

***MEK1* function is dependent upon dimerization.** Autophosphorylation can occur either intramolecularly (in *cis*) or between different Mek1 molecules (in *trans*). Autophosphorylation in *trans* could explain the role that Mek1 dimerization plays in creating the BSCR. Although a physical interaction between Mek1 molecules has yet to be demonstrated biochemically, a large body of genetic evidence exists to support this idea. First, when protein fusions are generated between Mek1 and different affinity tags, such as GST, LexA, or TAP, a correlation is observed between the ability of the fusion protein to suppress the *hop1-K593A* Hop1 C domain mutant and the ability of the tag to dimerize. Second, mutations that disrupt GST dimerization fail to suppress *hop1-K593A* but do not interfere with *MEK1* function (27). Third, *FKBP-MEK1* suppresses *hop1-K593A* only when dimerization is induced by addition of ligand. This experiment indicates that dimerization is the function directly responsible for bypassing the requirement of the Hop1 C domain in the BSCR. Fourth, a *HOP1*-dependent putative dimerization domain within Mek1 has been identified in a conserved region of the kinase located immediately downstream of the catalytic domain. Mutations within this domain are nonfunctional in untagged Mek1 but can be suppressed by ectopic dimerization conferred by GST.

Although our interpretation has focused on dimerization as a requirement for activation, an alternative possibility is that ectopic dimerization mediated by GST or FKBP raises the threshold concentration of the kinase above the level required for autophosphorylation to occur. This idea is supported by the observation that predimerized GST-*mek1* activation domain mutants exhibit higher levels of spore viability than untagged activation domain mutants. Biochemical detection of untagged Mek1 oligomers is necessary to distinguish between these two possibilities.

A model for Mek1 activation. GST-Mek1 exhibits T327 phosphorylation in a *hop1-K593A* mutant, indicating that ectopic dimerization can bypass the requirement for the Hop1 C domain. Dimerization alone, however, is insufficient for Mek1 kinase activation. Although GST-Mek1 is presumably constitutively dimerized in strains lacking DSBs or Hop1/Red1 or Red1/Mek1 complexes, no T327 phosphorylation is observed.

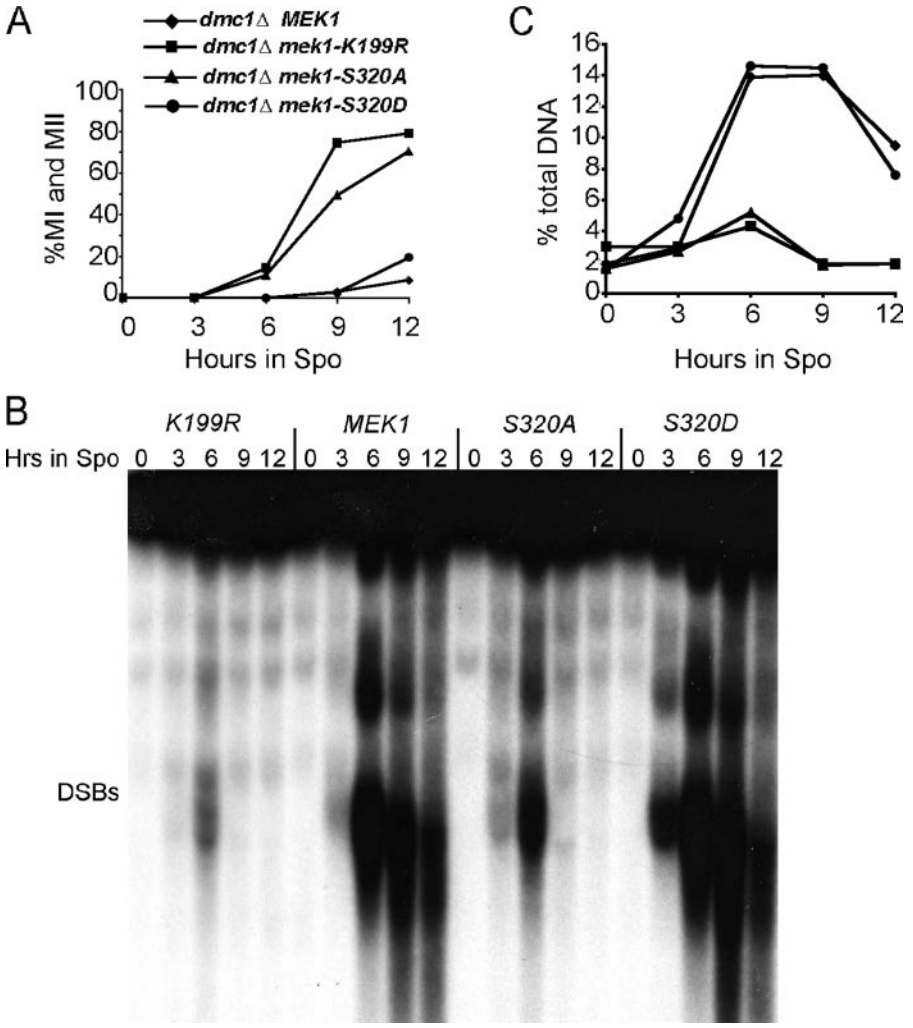

FIG. 6. Meiotic time course analysis of *mek1-S320A dmc1*Δ and *mek1-S320D dmc1*Δ mutants. *MEK1 dmc1*Δ (NH520::pLP37), *mek1-K199R dmc1*Δ (NH520::pLP36), *mek1-S142A S320A dmc1*Δ (NH520::pLP37-S320A), and *mek1-S320D dmc1*Δ (NH520::pLP37-S320D) mutants were transferred to Spo medium at 30°C, and samples were taken at 3-h intervals. (A). Meiotic progression measured by DAPI staining of cells to determine the fractions of binucleate (MI) and tetranucleate (MII) cells. Two hundred cells were counted for each strain at each time point. (B) DSBs detected at the *YCR048w* hotspot on chromosome III. (C) Quantitation of the DSB gel shown in panel B.

Therefore, dimerized Mek1 must be properly localized to Hop1/Red1 complexes to become activated, and this activation still requires DSBs. To explain these results, the following model for the regulation of Mek1 kinase activation is proposed. Hop1/Red1 complexes are bound to chromosomes prior to DSB formation, consistent with cytological data showing that both proteins localize to chromosomes in a *spo11*Δ mutant (40) (Fig. 7, step 1). DSBs result in phosphorylation of both Red1 and Hop1 (Fig. 7, step 2). Although DSB-dependent phosphorylation of Hop1 has been demonstrated (27), Red1 is already phosphorylated in the absence of breaks (L. Wan and N. M. Hollingsworth, unpublished results), and therefore DSB-dependent hyperphosphorylation of Red1 may be difficult to detect. Mek1 is then recruited to hyperphosphorylated Red1 via the Mek1 FHA domain (Fig. 7, step 3). Cytological experiments indicate that Mek1 colocalization with Red1 is dependent upon *SPO11* (and therefore DSBs), consistent with this idea (B. Rockmill, personal communication). Once bound, phosphorylated Hop1 C domains promote Mek1 dimerization (Fig. 7, step 4). Dimerization enables Mek1 kinase activation by autophosphorylation of T327 and T331 in *trans* (Fig. 7, step 5). The Mek1 FHA-phospho-Red1 interaction may be necessary to position the kinase molecules for autophosphorylation in the dimerized state. Once activated, the kinase must still be properly localized to function. *GST-mek1-R51A-T327D*, a constitutively active allele of Mek1 that is unable to bind to phospho-Red1, produces inviable spores (C. Park and N. M. Hollingsworth, unpublished results). Proper Mek1 localization may be necessary for phosphorylation of target proteins.

Our model for Mek1 activation in response to DSBs shares similarities with activation of the checkpoint kinase Rad53 in response to DNA damage (31). Mek1 resembles Rad53 in being a kinase with an FHA domain (although Rad53 has two). When DNA damage occurs in vegetative cells, Mec1 kinase is activated and phosphorylates Rad9 (37). FHA domains on

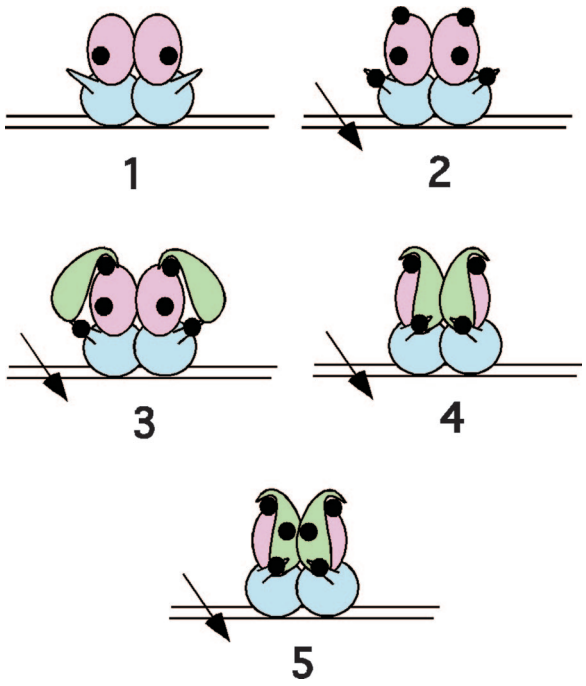

FIG. 7. Model for Mek1 activation in response to meiotic DSBs. 1, Hop1/phospho-Red1 complexes are assembled onto chromosomes prior to DSB formation; 2, introduction of a DSB results in phosphorylation of the C domains of Hop1 molecules in the region of the breaks and additional phosphorylation of Red1; 3, DSB-specific phospho-amino acids on Red1 allow recruitment of Mek1 via the FHA domain; 4, phosphorylated Hop1 C domains promote dimerization of Mek1; 5, Mek1 is activated by autophosphorylation in *trans* of the activation loop. Blue, Hop1; green, Mek1; red, Red1. Arrows indicate DSBs. Black circles indicate phosphates. Double lines indicates a DNA duplex of a chromatid.

Rad53 bind to phosphothreonines on Rad9, which serves as an adaptor protein that allows Mec1 phosphorylation of Rad53 (41). Binding to Rad9 increases the local concentration of Rad53, thereby allowing autophosphorylation in *trans* (10). The *Schizosaccharomyces pombe* ortholog of Rad53, Cds1, similarly requires multiple steps for activation. In this case, Cds1 is recruited to DNA damage by binding Mrc1, after Mrc1 has been phosphorylated by Rad3 (the *S. pombe* Mec1 ortholog). Both phosphorylation of Cds1 by Rad3 and dimerization-induced autophosphorylation in *trans* of threonines in the activation domain are then required for Cds1 activation (50). Unlike the case for Rad53 and Cds1, however, phosphorylation by other kinases outside the activation segment does not appear to be necessary for Mek1 activation. MS of Mek1 purified from meiotic cells detected only four phospho-amino acids. Of these, phosphorylation of T327 and T331 is required for activation, S320 is required only under *dmc1*Δ-arrested conditions, and S142 has no obvious phenotypes. Nevertheless, it is intriguing to note that similar mechanisms for kinase activation may either promote repair of DNA damage in vegetative cells (Rad53 and Cds1) or suppress intersister recombination in meiotic cells (Mek1).

Additional phosphorylation of the activation domain is required to maintain the BSCR in *dmc1*Δ-arrested cells. MS revealed an additional phosphorylation site with a previously unsuspected role in meiosis. S320 is located within the Mek1 activation domain (Fig. 1). Replacement of Mek1 S320 with alanine results in no apparent phenotypes in an otherwise wild-type diploid but allows *dmc1*Δ diploids to sporulate. The failure of *mek1-S320A dmc1*Δ cells to arrest could result from bypassing the need for *DMC1* in interhomolog recombination, as has been observed either when *RAD51* or *RAD54* is overexpressed or when *HED1* is deleted (5, 43, 44). In these situations, interhomolog recombination enables proper meiotic chromosome segregation and the production of viable spores. The spores produced in *dmc1*Δ strains containing *mek1-S320A* are dead, however, ruling out this explanation. Alternatively, phosphorylation of S320 could be required for *MEK1* to function in the meiotic recombination checkpoint (35, 49). In this case, disruption of the checkpoint would allow meiotic progression without DSB repair, producing dead spores as a result of broken chromosomes. However, DSBs are efficiently repaired in *mek1-S320A dmc1*Δ diploids, indicating that the meiotic progression observed in this strain is not due to a defect in Mek1's checkpoint function but instead to the failure of Mek1 to create a BSCR. The *dmc1*Δ arrest and unrepaired breaks are restored if S320 is replaced with a phosphomimetic amino acid, demonstrating that a negative charge at this position is necessary for *MEK1* function under these conditions. *mek1-S320A* is therefore defective in suppressing intersister DSB repair, but only when cells are arrested by the absence of *DMC1*.

Ectopic dimerization bypasses the need for S320 phosphorylation, as addition of *GST* to *mek1-S320A* restores the *dmc1*Δ arrest. Phosphorylation of S320 could promote the initial dimerization of Mek1 in response to DSBs. However this seems unlikely given that *mek1-S320A* alone produces highly viable spores and therefore must be capable of generating a BSCR in otherwise wild-type cells. A more likely explanation is that phosphorylation of S320 is required to maintain Mek1 in the dimerized state after a BSCR has been established. Inactivation of Mek1-as by addition of inhibitor to a *mek1-as dmc1*Δ diploid results in a rapid repair of DSBs, indicating that Mek1 must be constitutively active to prevent Rad51-mediated strand invasion of sister chromatids during meiosis (45). The requirement for dimerized, active Mek1 may be relatively brief in wild-type cells, where the need for a BSCR is removed once strand invasion of the homolog has occurred. In contrast, the prolonged arrest triggered by *dmc1*Δ may require continuous reinforcement of the dimerized and active state for Mek1, a process facilitated by phosphorylation of S320. Consistent with this idea, *GST-mek1-T327D* has sufficient activity to create viable spores in an otherwise wild-type meiosis but has a level of activity insufficient to maintain *dmc1*Δ arrest. The maintenance of the dimerized state may be necessary either because phosphatase removal of the T327 and T331 phosphates requires continuous autophosphorylation to keep Mek1 activated or because dimerized Mek1 is necessary for efficient phosphorylation of the target proteins that create the BSCR.

In summary, phosphorylation plays a key role in suppressing DSB repair between sister chromatids during meiosis. Hop1 is a DSB-dependent phosphoprotein, and Mek1 recruitment to Hop1/Red1 complexes requires phospho-Red1. Once dimerized, Mek1 activates itself by autophosphorylation of conserved residues in the activation loop. Maintenance of the

dimerized state may require additional phosphorylation of the activation loop; whether this would be by Mek1 or another kinase is not yet clear. Finally, Mek1 phosphorylation of unknown proteins specifically suppresses intersister DSB repair in meiosis.

ACKNOWLEDGMENTS

We thank Aaron Neiman for helpful discussions and comments on the manuscript and Doug Kellogg for GST antibodies. We are grateful to Beth Rockmill for sharing unpublished results.

This work was supported by National Institutes of Health grants GM50717 (to N.M.H.), HG3456 (to S.P.G.), and GM61641 (to D.M.).

REFERENCES

1. **Adams, J. A.** 2003. Activation loop phosphorylation and catalysis in protein kinases: is there functional evidence for the autoinhibitor model? Biochemistry **42:**601–607.
2. **Allers, T., and M. Lichten.** 2001. Differential timing and control of noncrossover and crossover recombination during meiosis. Cell **106:**47–57.
3. **Bailis, J. M., and G. S. Roeder.** 1998. Synaptonemal complex morphogenesis and sister-chromatid cohesion require Mek1-dependent phosphorylation of a meiotic chromosomal protein. Genes Dev. **12:**3551–3563.
4. **Bishop, D. K.** 1994. RecA homologs Dmc1 and Rad51 interact to form multiple nuclear complexes prior to meiotic chromosome synapsis. Cell **79:**1081–1092.
5. **Bishop, D. K., Y. Nikolski, J. Oshiro, J. Chon, M. Shinohara, and X. Chen.** 1999. High copy number suppression of the meiotic arrest caused by a *dmc1* mutation: *REC114* imposes an early recombination block and *RAD54* promotes a *DMC1*-independent DSB repair pathway. Genes Cells **4:**425–443.
6. **Bishop, D. K., D. Park, L. Xu, and N. Kleckner.** 1992. *DMC1*: a meiosis-specific yeast homolog of *E. coli recA* required for recombination, synaptonemal complex formation and cell cycle progression. Cell **69:**439–456.
7. **Brachmann, C. B., A. Davies, G. J. Cost, E. Caputo, J. Li, P. Hieter, and J. D. Boeke.** 1998. Designer deletion strains derived from *Saccharomyces cerevisiae* S288C: a useful set of strains and plasmids for PCR-mediated gene disruption and other applications. Yeast **14:**115–132.
8. **Cheng, H., T. Addona, H. Keshishian, E. Dahlstrand, C. Lu, M. Dorsch, Z. Li, A. Wang, T. D. Ocain, P. Li, T. F. Parsons, B. Jaffee, and Y. Xu.** 2007. Regulation of IRAK-4 kinase activity via autophosphorylation within its activation loop. Biochem. Biophys. Res. Commun. **352:**609–616.
9. **de los Santos, T., and N. M. Hollingsworth.** 1999. Red1p: A *MEK1*-dependent phosphoprotein that physically interacts with Hop1p during meiosis in yeast. J. Biol. Chem. **274:**1783–1790.
10. **Gilbert, C. S., C. M. Green, and N. F. Lowndes.** 2001. Budding yeast Rad9 is an ATP-dependent Rad53 activating machine. Mol. Cell **8:**129–136.
11. **Haas, W., B. K. Faherty, S. A. Gerber, J. E. Elias, S. A. Beausoleil, C. E. Bakalarski, X. Li, J. Villen, and S. P. Gygi.** 2006. Optimization and use of peptide mass measurement accuracy in shotgun proteomics. Mol. Cell Proteomics **5:**1326–1337.
12. **Hassold, T., and P. Hunt.** 2001. To err (meiotically) is human: the genesis of human aneuploidy. Nat. Rev. **2:**280–291.
13. **Hollingsworth, N. M., and S. J. Brill.** 2004. The Mus81 solution to resolution: generating meiotic crossovers without Holliday junctions. Genes Dev. **18:**117–125.
14. **Hollingsworth, N. M., and A. D. Johnson.** 1993. A conditional allele of the *Saccharomyces cerevisiae HOP1* gene is suppressed by overexpression of two other meiosis-specific genes: *RED1* and *REC104*. Genetics **133:**785–797.
15. **Hollingsworth, N. M., L. Ponte, and C. Halsey.** 1995. *MSH5*, a novel MutS homolog, facilitates meiotic reciprocal recombination between homologs in *Saccharomyces cerevisiae* but not mismatch repair. Genes Dev. **9:**1728–1739.
16. **Hunter, N., and N. Kleckner.** 2001. The single-end invasion: an asymmetric intermediate at the double-strand break to double-Holliday junction transition of meiotic recombination. Cell **106:**59–70.
17. **Huse, M., and J. Kuriyan.** 2002. The conformational plasticity of protein kinases. Cell **109:**275–282.
18. **Johnson, L. N., M. E. M. Noble, and D. J. Owen.** 1996. Active and inactive protein kinases: structural basis for regulation. Cell **19:**149–158.
19. **Kadyk, L. C., and L. H. Hartwell.** 1992. Sister chromatids are preferred over homologs as substrates for recombinational repair in *Saccharomyces cerevisiae*. Genetics **132:**387–402.
20. **Kaldis, P., A. Sutton, and M. J. Solomon.** 1996. The Cdk-activating kinase (CAK) from budding yeast. Cell **86:**553–564.
21. **Keeney, S.** 2001. Mechanism and control of meiotic recombination initiation. Curr. Top. Dev. Biol. **52:**1–53.
22. **Li, W., and W. T. Miller.** 2006. Role of the activation loop tyrosines in regulation of the insulin-like growth factor I receptor-tyrosine kinase. J. Biol. Chem. **281:**23785–23791.
23. **Li, X., S. A. Gerber, A. D. Rudner, S. A. Beausoleil, W. Haas, J. Villen, J. E. Elias, and S. P. Gygi.** 2007. Large-scale phosphorylation analysis of alpha-factor-arrested *Saccharomyces cerevisiae*. J. Proteome Res. **6:**1190–1197.
24. **Lydall, D., Y. Nikolsky, D. K. Bishop, and T. Weinert.** 1996. A meiotic recombination checkpoint controlled by mitotic checkpoint genes. Nature **383:**840–843.
25. **Marte, B. M., and J. Downward.** 1997. PKB/Akt: connecting phosphoinositide 3-kinase to cell survival and beyond. Trends Biochem. Sci. **22:**355–358.
26. **Neiman, A. M., and I. Herskowitz.** 1994. Reconstitution of a yeast protein kinase cascade *in vitro*: activation of the yeast MEK homolog STE7 by STE11. Proc. Natl. Acad. Sci. USA **91:**3398–3402.
27. **Niu, H., L. Wan, B. Baumgartner, D. Schaefer, J. Loidl, and N. M. Hollingsworth.** 2005. Partner choice during meiosis is regulated by Hop1-promoted dimerization of Mek1. Mol. Biol. Cell **16:**5804–5818.
28. **Nolen, B., S. Taylor, and G. Ghosh.** 2004. Regulation of protein kinases; controlling activity through activation segment conformation. Mol. Cell **15:**661–675.
29. **Paques, F., and J. E. Haber.** 1999. Multiple pathways of recombination induced by double-strand breaks in *Saccharomyces cerevisiae*. Microbiol. Mol. Biol. Rev. **63:**349–404.
30. **Pecina, A., K. N. Smith, C. Mezard, H. Murakami, K. Otha, and A. Nicolas.** 2002. Target stimulation of meiotic recombination. Cell **111:**173–184.
31. **Pellicioli, A., and M. Foiani.** 2005. Signal transduction: how rad53 kinase is activated. Curr. Biol. **15:**R769–R771.
32. **Peng, J., and S. P. Gygi.** 2001. Proteomics: the move to mixtures. J. Mass Spectrom. **36:**1083–1091.
33. **Petronczki, M., M. F. Siomos, and K. Nasmyth.** 2003. Un menage a quatre: the molecular biology of chromosome segregation in meiosis. Cell **112:**423–440.
34. **Prowse, C. N., and J. Lew.** 2001. Mechanism of activation of ERK2 by dual phosphorylation. J. Biol. Chem. **276:**99–103.
35. **Roeder, G. S., and J. M. Bailis.** 2000. The pachytene checkpoint. Trends Genet. **16:**395–403.
36. **Schwacha, A., and N. Kleckner.** 1995. Identification of double Holliday junctions as intermediates in meiotic recombination. Cell **83:**783–791.
37. **Schwartz, M. F., J. K. Duong, Z. Sun, J. S. Morrow, D. Pradhan, and D. F. Stern.** 2002. Rad9 phosphorylation sites couple Rad53 to the *Saccharomyces cerevisiae* DNA damage checkpoint. Mol. Cell **9:**1055–1065.
38. **Shinohara, A., and M. Shinohara.** 2004. Roles of RecA homologues Rad51 and Dmc1 during meiotic recombination. Cytogenet Genome Res. **107:**201–207.
39. **Sikorski, R. S., and P. Hieter.** 1989. A system of shuttle vectors and yeast host strains designed for efficient manipulation of DNA in *Saccharomyces cerevisiae*. Genetics **122:**19–27.
40. **Smith, A. V., and G. S. Roeder.** 1997. The yeast Red1 protein localizes to the cores of meiotic chromosomes. J. Cell Biol. **136:**957–967.
41. **Sweeney, F. D., F. Yang, A. Chi, J. Shabanowitz, D. F. Hunt, and D. Durocher.** 2005. *Saccharomyces cerevisiae* Rad9 acts as a Mec1 adaptor to allow Rad53 activation. Curr. Biol. **15:**1364–1375.
42. **Thompson, D. A., and F. W. Stahl.** 1999. Genetic control of recombination partner preference in yeast meiosis. Isolation and characterization of mutants elevated for meiotic unequal sister-chromatid recombination. Genetics **153:**621–641.
43. **Tsubouchi, H., and G. S. Roeder.** 2006. Budding yeast Hed1 down-regulates the mitotic recombination machinery when meiotic recombination is impaired. Genes Dev. **20:**1766–1775.
44. **Tsubouchi, H., and G. S. Roeder.** 2003. The importance of genetic recombination for fidelity of chromosome pairing in meiosis. Dev. Cell **5:**915–925.
45. **Wan, L., T. de los Santos, C. Zhang, K. Shokat, and N. M. Hollingsworth.** 2004. Mek1 kinase activity functions downstream of *RED1* in the regulation of meiotic DSB repair in budding yeast. Mol. Biol. Cell **15:**11–23.
46. **Wiltzius, J. J., M. Hohl, J. C. Fleming, and J. H. Petrini.** 2005. The Rad50 hook domain is a critical determinant of Mre11 complex functions. Nat. Struct. Mol. Biol. **12:**403–407.
47. **Woltering, D., B. Baumgartner, S. Bagchi, B. Larkin, J. Loidl, T. de los Santos, and N. M. Hollingsworth.** 2000. Meiotic segregation, synapsis, and recombination checkpoint functions require physical interaction between the chromosomal proteins Red1p and Hop1p. Mol. Cell. Biol. **20:**6646–6658.
48. **Wu, T.-C., and M. Lichten.** 1994. Meiosis-induced double-strand break sites determined by yeast chromatin structure. Science **263:**515–518.
49. **Xu, L., B. M. Weiner, and N. Kleckner.** 1997. Meiotic cells monitor the status of the interhomolog recombination complex. Genes Dev. **11:**106–118.
50. **Xu, Y. J., M. Davenport, and T. J. Kelly.** 2006. Two-stage mechanism for activation of the DNA replication checkpoint kinase Cds1 in fission yeast. Genes Dev. **20:**990–1003.
51. **Yves-Masson, J., and S. C. West.** 2001. The Rad51 and Dmc1 recombinases: a non-identical twin relationship. Trends Biochem. Sci. **26:**131–136.